



# Ball Burnishing For The Formation Of A Regular Helical Relief On Load-Bearing Surfaces Of Transport Machine Components

**Turaev Tirkash**

Associate Professor, Fergana State Technical University  
Republic of Uzbekistan, Fergana

*E-mail: tirkashturayev@gmail.com (+998 93 484 20 44)*

**Madaminov Bahrom  
Mirodilovich**

Associate Professor (PhD), Fergana State Technical University  
Republic of Uzbekistan, Fergana

*E-mail: madamin1541208@gmail.com (+998 93 733 53 04)*

## ABSTRACT

The process of external ball burnishing for the formation of a regular helical relief on the load-bearing surfaces of transport machine components is considered. Based on Hertzian contact theory, the conditions for plastic deformation of the surface layer are established, and estimates of strengthening are provided. The formation of compressive residual stresses in steel 20 is confirmed, ensuring an increase in the fatigue strength of the components.

## Keywords:

Ball burnishing; surface strengthening; helical microrelief; Hertzian contact; plastic deformation; residual stresses; steel 20.

## Introduction.

The present study examines the process of external ball burnishing used to form a regular helical relief on the load-bearing surfaces of transport machine components manufactured as bodies of revolution.

The process is based on the contact interaction between a rotating ball tool and the workpiece surface under axial or helical feed of the part. Under the action of the normal force ( $F$ ), a localized stress-strain state arises in the contact zone, leading to plastic deformation of the surface layer.

The kinematic scheme of the coupled process can be represented as follows: ball (rotation)  $\rightarrow$  contact interaction ( $F, H$ )  $\rightarrow$  workpiece (body of revolution, feed).

As a result of the process, the following effects occur:

- plastic flattening of surface microroughness (asperities);

- formation of a regular helical microrelief;
- strengthening of the surface layer due to strain hardening;
- generation of compressive residual stresses that increase the fatigue strength of the component.

The application of ball burnishing improves the operational characteristics of load-bearing surfaces of transport machine components, including wear resistance, contact fatigue resistance, and resistance to fatigue failure, without material removal and with minimal energy consumption.

## Methods.

**Calculation scheme and contact interaction (based on Hertzian theory).** The process of external ball burnishing is carried out using a rotating ball tool in contact with the surface of a workpiece manufactured as a body of revolution. The workpiece is subjected to

axial or helical feed, resulting in the formation of a regular helical relief on its surface.

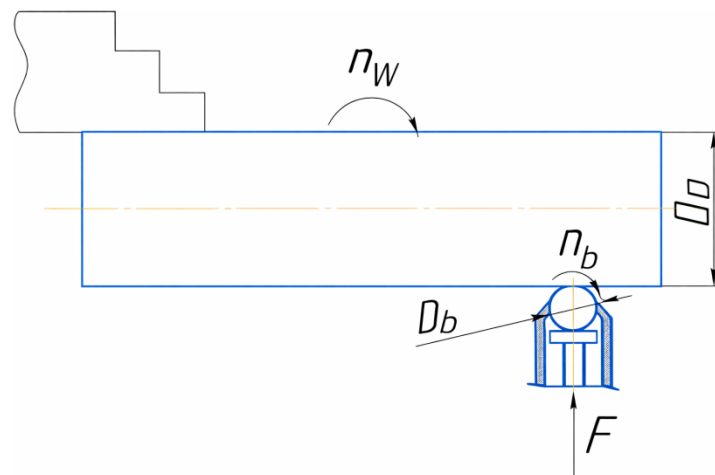


**Fig. 1. Calculation scheme of the component:**

1. Ball of diameter ( $D_b$ ); 2. Workpiece – cylinder of diameter ( $D_d$ ); 3. Contact zone with radius ( $a$ ); 4. Normal pressing force ( $F$ ); 5. Direction of ball rotation; 6. Feed direction ( $S$ ); 7. Helical deformation trajectory line; 8. Spindle rotational speed ( $n_d$ ).

Ball burnishing belongs to the methods of surface plastic deformation, in which processing is carried out without material removal and is accompanied by strengthening of the surface layer [2]. The method is widely used to improve wear resistance and fatigue strength of load-bearing surfaces of transport machine components.

The process is realized through the contact interaction of a rotating ball tool with the surface of a component manufactured as a body of revolution. The workpiece is subjected to axial or helical feed, which leads to the formation of a regular helical microrelief.

To evaluate the stress state in the contact zone, Hertzian elastic contact theory is applied [1,5]. For the contact between a ball and a cylindrical component, the reduced radius of curvature is determined by the following expression:

$$\rho_{eq} = \frac{1}{R_b} + \frac{1}{R_w} = \frac{2}{R_b} + \frac{2}{R_w}$$

or

$$\rho_{eq} = \frac{D_b \cdot D_w}{2(D_b + D_w)}$$

**where:**  $D_b$  – ball diameter;  $D_w$  – workpiece diameter.

The reduced elastic modulus of the contacting pair of materials ( $E'$ ), taking into account Poisson's ratio ( $\nu$ ), is calculated by the following formula:

$$\frac{1}{E'} = \frac{1-\nu_1^2}{E_1} + \frac{1-\nu_2^2}{E_2}$$

For the case of homogeneous materials (steel–steel), the expression is simplified as follows:

$$E' = \frac{E}{2(1-\nu^2)}$$

Under the action of the normal pressing force  $F$ , a contact area is formed. The radius of the contact area  $a$  is calculated as follows:

$$a = \sqrt{\frac{3F\rho_{eq}}{4E'}}$$

The maximum contact stress  $\sigma_{max}$  at the center of the contact area is determined by the following relationship:

$$\sigma_{max} = \frac{3F}{2\pi a^2}$$

**Numerical example** (workpiece material: steel 20; ball material: bearing steel ШХ15).  
 Let:  $D_b = 10$  mm;  $D_w = 40$  mm;  $F = 300$  N;  $E = 2.1 \cdot 10^5$  MPa;  $\nu = 0.3$ ;  
 then:  $R' \approx 3.3$  mm;  $E' \approx 1.15 \cdot 10^5$  MPa;  $a \approx 0.85$  mm.

**The maximum contact stress:**

$$\sigma_{max} = \frac{(3 \cdot F)}{(2\pi)a^2}, \quad \sigma_{max} \approx 3.5hPa$$

The obtained value exceeds the yield strength of steel 20 ( $\sigma_y \approx 245$  MPa), which ensures plastic deformation of the surface layer. Plastic flattening of surface asperities occurs: the initial surface roughness after turning is  $Ra_0 = 3.2$   $\mu$ m, and after ball burnishing with three passes it is reduced to  $Ra_1 = 0.2 \div 0.4$   $\mu$ m. The depth of deformation  $\varepsilon$ , i.e., the relative plastic deformation of surface asperities after burnishing with a steel ball head, is determined by the following formula:

$$\varepsilon = \left[ \frac{(Ra_0 - Ra_1)}{Ra_0} \right] \cdot 100\% = \left[ \frac{3.2 - 0.3}{3.2} \right] \cdot 100\% \approx 90\%$$

**Results.**

The following calculated data were obtained:

- reduced radius –  $\rho_{eq} = 3.33$  mm;
- reduced elastic modulus –  $E' \approx 1.15 \cdot 10^5$  MPa;
- contact radius –  $a \approx 0.086$  mm;
- maximum stress –  $\sigma_{max} \approx 6.4$  hPa.

This confirms intensive smoothing of the microprofile without material removal. During burnishing, the depth of the relatively hardened layer is estimated as:  $h_p \approx 0.25 - 0.45$  mm

Substituting the value of ( $a$ ) in terms of the force ( $F$ ), the following relationship is obtained:  $h = k \cdot F$  [3].

No	Burnishing force F, (N)	Indentation radius (a), mm	Depth of hardening (h), mm
1	100	0,060	0,042
2	200	0,075	0,053
3	300	0,086	0,061
4	400	0,095	0,067
5	500	0,102	0,072

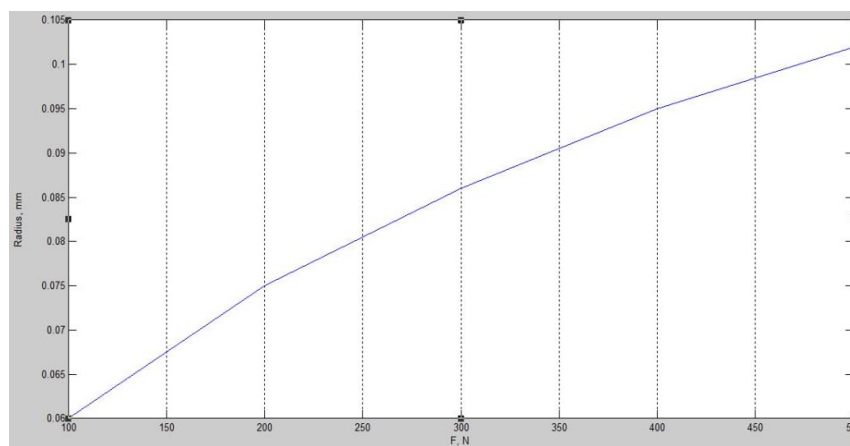


**Fig. 2. Dependence of the depth of the plastically deformed layer ( $h$ ) on the normal pressing force ( $F$ ) during burnishing with a steel ball of diameter  $D_b=10$  mm. The graphs show the calculated behavior for steel 20. The plots were obtained using a MATLAB-based method ( $4/h$ )**

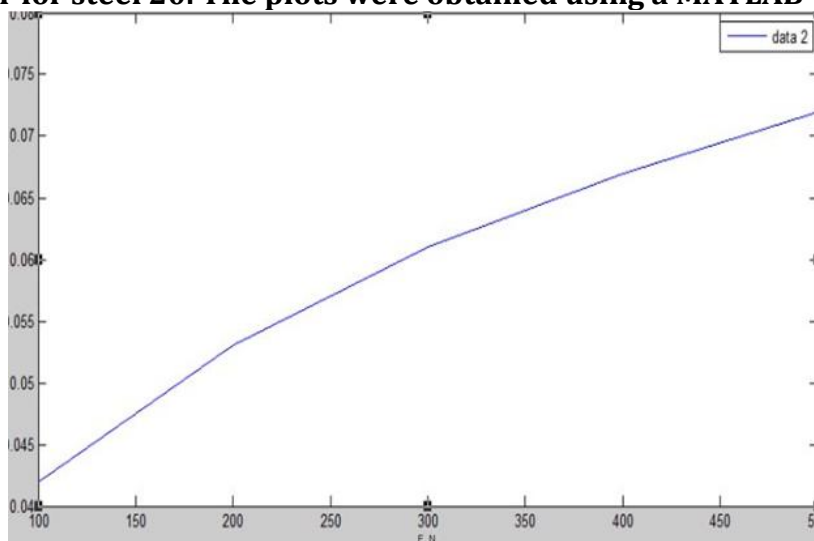


**Fig. 3. Dependence of the depth of the plastically deformed layer ( $h$ ) on the normal pressing force ( $F$ ) during burnishing with a steel ball of diameter  $D_b=10$  mm. The graphs show the calculated behavior for steel 40X. The plots were obtained using a MATLAB-based method ( $4/h$ )**

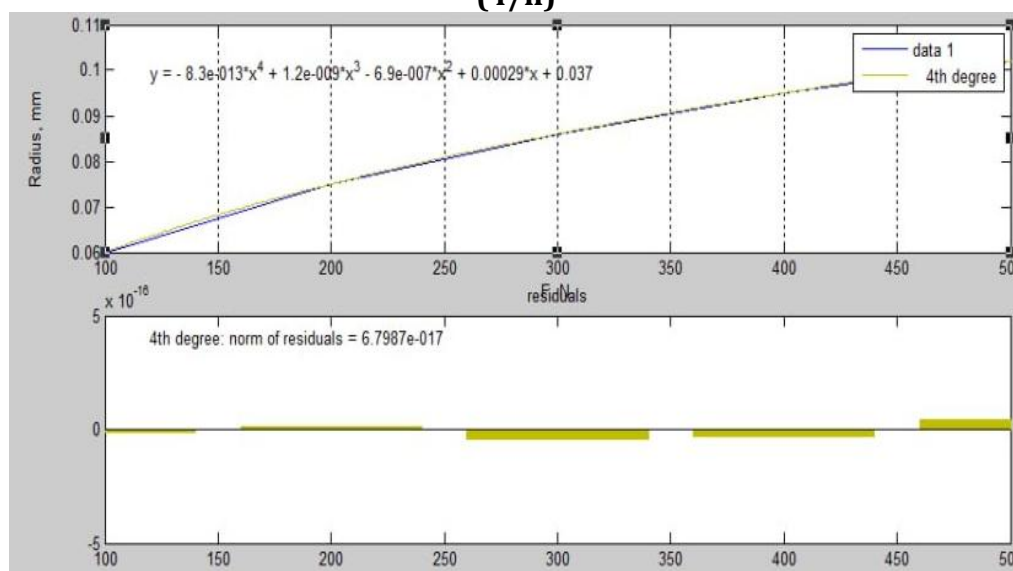


**Fig. 4. Formula used for constructing the graphs generated in MATLAB**

Analysis of the  $h = f(F)$  relationship shows that increasing the burnishing force from 100 N to 500 N leads to a nonlinear growth of the depth of the hardened layer. The most intensive increase is observed in the range up to 300 N. Further increase in force (above 500 N) with a small ball diameter ( $D_b = 10$  mm) is impractical, as it may lead to over-hardening of the surface and the formation of microcracks (“peeling”) due to excessive contact stresses exceeding the material strength limit.

For load-bearing surfaces of transport machine components, this value is considered optimal, as it exceeds the depth of maximum contact stresses occurring during operation.

The formation of a regular helical microrelief is achieved through the kinematic superposition of the rotation of the workpiece and the axial feed of the ball tool. The pitch ( $t$ ) and the helix angle ( $\alpha$ ) of the helical relief are determined by the processing parameters and remain constant along the entire length of the machined surface.

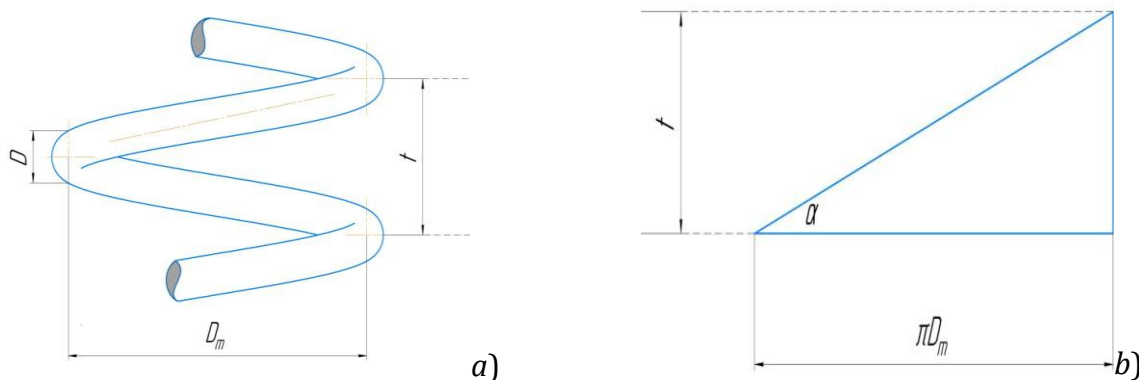


**Fig. 5. Schemes for determining the pitch  $t$  (a) and the helix angle ( $\alpha$ ) of the helical relief (b).**

**where:**

$S$  – feed, mm/rev;

$n$  – rotational speed of the workpiece, rpm;

$D_b$  – distance traveled by the ball along the helix generatrix, mm;

$D_{im}$  – diameter of the ball indentation under the helical burnishing conditions, mm.

**Discussion.**

The presence of a helical microrelief promotes lubricant retention, reduces the coefficient of friction, and increases the contact fatigue resistance of load-bearing surfaces of transport machine components [2].

At  $S = 0.15$  mm/rev, a stable regular microrelief is formed, with asperities of a “sand-like” morphology, providing lubricant retention, reduction of the friction coefficient, and improvement of contact endurance.

The helical microrelief is formed after burnishing (for example, during machining of a cylindrical workpiece), when the ball rotates and moves with a feed ( $S$ ). A schematic representation is shown in Fig. 6.

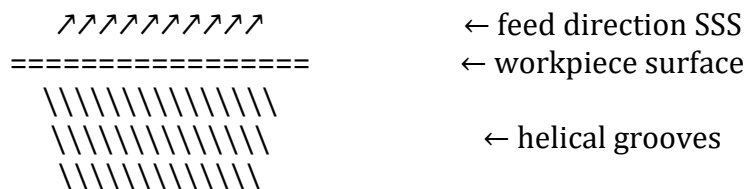


**Fig. 6. Schematic representation of helical formation.**

The main parameters of the helical relief are as follows: pitch of the relief ( $t$ ) feed per revolution, mm/rev; depth of the hardened layer ( $h$ )  $\approx 0.1 \div 0.4$  mm; surface roughness after burnishing:  $Ra \approx 0.4 \div 0.8 \mu\text{m}$ .

A regular plastically deformed relief is formed.

**Surface**

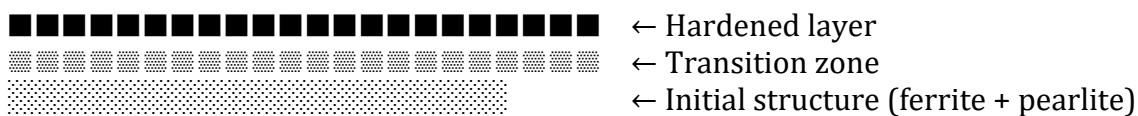


**Fig. 7. Schematic representation of helical formation.**

The helical shape is formed due to the combination of: rotation of the workpiece, axial feed of the tool, and pressure of the ball on the surface.

Structure of steel 20 before processing. Steel 20 is a low-carbon structural steel ( $\approx 0.2\% \text{ C}$ ). Before burnishing, its structure consists of: ferrite ( $\alpha\text{-Fe}$ ) – light regions; pearlite – dark regions. This is a typical ferrite–pearlite structure prior to ball burnishing.

### Microstructure after ball burnishing

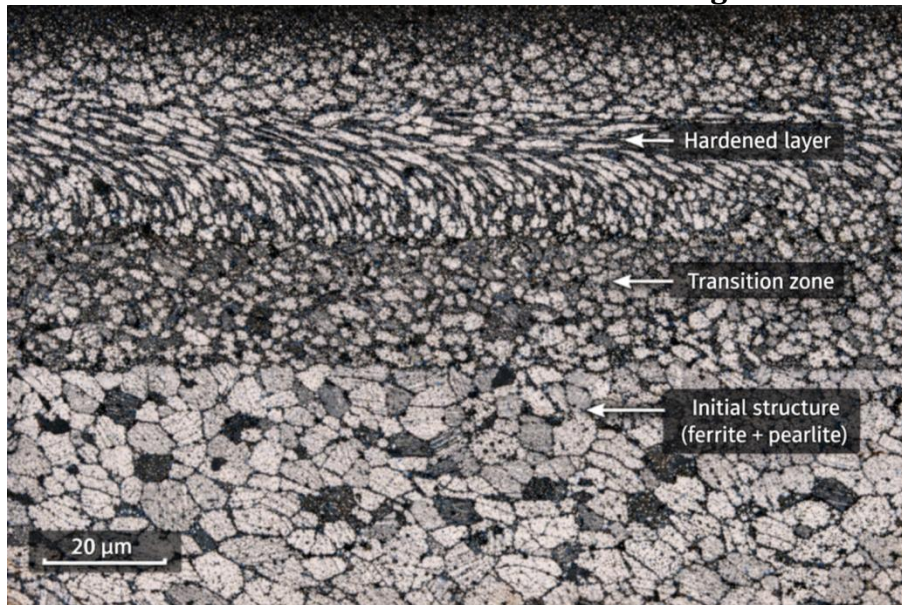


**Fig. 8. Microstructure of steel grade 20 after ball burnishing. The 20  $\mu\text{m}$  scale bar indicates the dimensional scale, not the magnification of the structure.**

From the microstructure, it is observed that ferrite grains are elongated in the direction of deformation, while pearlite colonies become more compact. The microrelief in the micrograph is characterized by helical ridges with a height of 5–15  $\mu\text{m}$  and a uniform pitch. Strain hardening is formed: the dislocation density increases, and compressive residual

$$\sigma_{\text{res}} = (-200) \text{ to } (-350) \text{ MPa}$$

**where:**

“–” denotes compression.

### Effect on fatigue strength.

The endurance limit during burnishing with a steel ball:

$$\sigma_{-1} \text{ before } \approx 180 \text{ MPa}; \sigma_{-1} \text{ after } \approx 240\text{--}270 \text{ MPa.}$$

Increase in fatigue strength:  $K = 1.3 \div 1.5$

### Conclusions:

1. Ball burnishing ensures guaranteed plastic deformation of the surface layer.
2. A regular helical microrelief with a specified pitch is formed.
3. The depth of the hardened layer reaches up to 0.45 mm.
4. Microhardness increases by up to 40%.
5. Compressive residual stresses up to –350 MPa increase fatigue strength by up to 1.5 times.

### References:

1. Гуляев А.П. *Металловедение*. – М.: Машиностроение, 2011. – 640 с.
2. Соколов Л.А., Иванов В.И. *Поверхностное пластическое деформирование деталей машин*. – М.: Машиностроение, 2008. – 320 с.
3. Кудрявцев И.В. *Контактные напряжения и теория Герца*. – М.: Наука, 2005. – 256 с.

4. Гольдштейн Р.В. Остаточные напряжения и усталость металлов. – М.: Металлургия, 2006. – 280 с.
5. ГОСТ 2789–73. Шероховатость поверхности. Параметры и характеристики. – М.: Стандартиформ, 2019.
6. Turaev T., Ulugkhozhaev R. S., & Madaminov B. M. Technological Features Hardening Of The Case Of The Roller Track Of The Transport Machine By Ball Knurling Tool And Cartooning With Microballs Library Progress International, Vol.44 No.3, Jul-Dec 2024: P.7709-7719
7. Turaevich, T. T., & Mirodilovich, M. B. (2020). Physical Foundations Structural-Formation, Surface Layer Of Parts. *The American Journal of Engineering and Technology*, 2(09), 71-76.
8. Тураев, Т. Т., Батиров, Я. А., & Мадаминов, Б. М. (2021). Сравнительной оценки технического уровня станков и станочных систем. *Збірник наукових праць Л'ОГОЕ*.
9. Turaevich, T. T., Anvarhodjaevich, B. Y., & Mirodilovich, M. B. (2021). Choosing the optimal processing method to improve the productivity of machine tools and machine systems. *International Journal of Multicultural and Multireligious Understanding*, 8(5), 490-494.
10. Тураев, Т. Т., Акрамов, М. М., & Мадаминов, Б. М. (2023). ИЗУЧЕНИЯ ЭНЕРГЕТИЧЕСКОГО БАЛАНСА ПРИ ИСПОЛЬЗОВАНИЯ МЕТОДА ОБРАБОТКИ ПОВЕРХНОСТНЫМ ПЛАСТИЧЕСКИМ ДЕФОРМИРОВАНИЕМ. *European Journal of Interdisciplinary Research and Development*, 14, 290-295.
11. Turayevich, T. T., Adiljonovich, E. D., & Mirodilovich, M. B. (2022). IMPROVING THE DURABILITY OF COMPRESSOR EQUIPMENT PARTS IN THE CHEMICAL AND PETROCHEMICAL INDUSTRIES.